# MS/MS Sequencing of Digitally Encoded Poly(alkoxyamine amide)s

**ARTICLE** *in* MACROMOLECULES · JULY 2015

Impact Factor: 5.8 · DOI: 10.1021/acs.macromol.5b01051



**4 AUTHORS:**

Laurence Charles
Aix-Marseille Université
**134** PUBLICATIONS **1,121** CITATIONS
SEE PROFILE

Chloé Laure
University of Strasbourg
**5** PUBLICATIONS **23** CITATIONS
SEE PROFILE

Jean-François Lutz
French National Centre for Scientific Research
**179** PUBLICATIONS **9,002** CITATIONS
SEE PROFILE

Raj Kumar Roy
Nagoya University
**10** PUBLICATIONS **74** CITATIONS
SEE PROFILE

Macromolecules

Article

pubs.acs.org/Macromolecules

# MS/MS Sequencing of Digitally Encoded Poly(alkoxyamine amide)s

Laurence Charles,*[,†] Chloé Laure,[‡] Jean-François Lutz,*[,‡] and Raj Kumar Roy[‡]

[†]Aix-Marseille Université − CNRS, UMR 7273, Institute of Radical Chemistry, 13397 Marseille Cedex 20, France

[‡]Precision Macromolecular Chemistry, UPR22-CNRS, BP84047, Institut Charles Sadron, 23 rue du Loess, 67034 Strasbourg, Cedex 2, France

Supporting Information

**ABSTRACT:** Monodisperse sequence-coded oligo(alkoxyamine amide)s were thoroughly investigated by tandem mass spectrometry to evaluate the robustness of this analytical approach as a reliable sequencing methodology. Studied samples were synthesized by orthogonal iterative chemistry on a solid support, and the 0/1 coding system was based on the mass of two amide synthons that alternate with a nitroxide moiety. The major fragmentation pathway experienced by these co-oligomers proceeded via homolysis of all fragile C−ON bonds between a coding unit and a nitroxide moiety. The relative rate of competing C−ON bond cleavages was observed to be sequence-dependent, offering an additional means to validate the sequences reconstructed from the MS/MS fragments. The same fragmentation rules applied for all studied samples, varying in terms of chain length, charge state, encoded sequence, end-groups, and nitroxide moiety. Ion mobility separation was coupled to MS/MS to sequence some more complex co-oligomers composed of both different nitroxides and coding units.

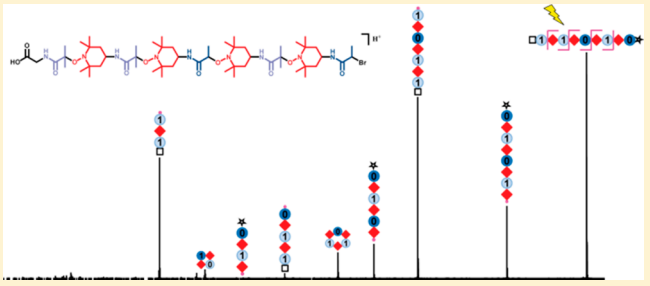

## INTRODUCTION

Information-containing macromolecules are polymers that contain a message encoded by a defined sequence of monomers.[1] DNA contains for example genetic information coded by nucleotides. Very recently, it was also proposed that synthetic polymers can also store intentionally written information.[2] For instance, a digital code can be implemented in a synthetic macromolecule using two comonomers defined as 0 and 1 bits. This concept was demonstrated with artificial DNA strands[3−5] but also using non-natural polymers.[6] For instance, the Lutz group has shown that digital information can be encrypted in polyphosphates,[7] oligo(triazole amide)s,[8−10] and oligo(alkoxyamine amide)s.[11] These polymers are prepared by sequential monomer-by-monomer synthesis on solid or soluble supports.[1] As a consequence, the formed polymers are perfectly monodisperse and sequence-defined.

For instance, oligo(alkoxyamine amide)s are synthesized using an orthogonal protecting-group-free iterative approach.[12] In this strategy, two successive chemoselective steps are used to prepare the polymers as depicted in Figure 1.[11] In the first step (noted (i) in Figure 1), a primary amine is reacted with a noncyclic symmetric anhydride to afford an amide. In the second step (noted (ii) in Figure 1), a carbon-centered radical, obtained by Cu(I) activation of an alkyl bromide, is coupled with a nitroxide to afford an alkoxyamine.[13] This method allows fast and facile synthesis of sequence-encrypted oligo(alkoxyamine amide)s. For instance, the use of two interchangeable anhydrides in the first step permits to implement a binary monomer code in the formed polymers. It is important to specify that this code is based on the molar mass of the amide synthons that compose the polymer chains (i.e., **0** = 71.0 Da and **1** = 85.1 Da) and not on their configuration. In other words, the monomer-based language is purely based on comonomer sequences and not on tacticity or secondary structure. Overall, it was found that oligo(alkoxyamine amide)s constitute a very interesting class of information-containing macromolecules. In particular, it was evidenced that the monomer-coded messages stored in their chains can be easily erased via temperature-triggered degradation.[11]

The success of any strategy used to encrypt information in synthetic copolymers also relies on the methodology to be implemented for reading their encoded messages, which is typically a sequencing task.[14] Tandem mass spectrometry (MS/MS) has long proved its efficiency and reliability when dealing with biopolymer sequencing. However, in contrast to peptides[15] or oligosaccharides[16] obeying universal dissociation rules that allow their automated sequencing from MS/MS spectra, fragmentation patterns of synthetic species strongly depend on the chemistry of the polymer backbone.[17] In fact, analysis of MS/MS data obtained upon collisional activation of molecules involving two comonomers might not always be simply performed by combining rules reported for corresponding homopolymers. As a result, only a few non-natural sequence-defined polymers have been studied so far by tandem mass spectrometry.[18−20] Ideally, MS/MS data should be easy to

Received: May 15, 2015
Revised: June 11, 2015

  

DOI: 10.1021/acs.macromol.5b01051
Macromolecules XXXX, XXX, XXX−XXX

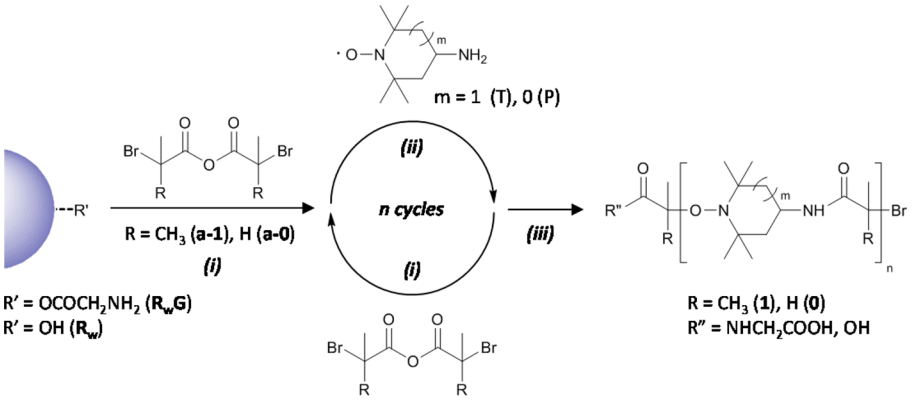


**Figure 1.** Iterative synthesis of sequence-coded oligo(alkoxyamine amide)s.[11] This strategy involves two successive orthogonal reactions: (i) primary amine−anhydride coupling and (ii) nitroxide radical coupling. The interchangeable use of two different anhydrides **a-1** and **a-0** in step (i) allows creation of a controlled digital sequence. The blue half-sphere represents a cross-linked polystyrene solid support. Experimental conditions: (i) base, THF, RT; (ii) CuBr, $Me_6$TREN, DMSO or THF, RT or microwave at 40 °C; (iii) TFA, $CH_2Cl_2$.

read and dissociation rules should be robust; i.e., they should neither vary as a function of the sequence nor of the end-groups. It was recently found that sequence-coded oligo(alkoxyamine amide)s fulfill these criteria and are remarkably easy to sequence by MS/MS.[11] Because of the labile alkoxyamine linkages within their backbone, poly(alkoxyamine amide)s happened to readily dissociate upon collisional activation via competitive homolytic cleavages of the C−ON bonds. As a result, quite simple dissociation rules could be established for these copolymers, allowing their sequencing in a straightforward manner. Hence, this novel class of polymers is particularly appealing for information-related applications such as data storage or anticounterfeit technologies. In the present article, the MS/MS sequencing of coded oligo(alkoxyamine amide)s is examined in detail. In particular, the dissociation mechanism of these polymers was studied using a broad range of model samples. This article gives further insights into the sequencing of non-natural macromolecules, which is a topic of increasing importance in fundamental polymer science.[14]

## EXPERIMENTAL SECTION

**Chemicals.** To prepare samples to be subjected to electrospray ionization (ESI), methanol was purchased from SDS (Peypin, France) and ammonium acetate was from Sigma-Aldrich (Saint Louis, MO). Poly(ethylene glycol) (PEG) and poly(methyl methacrylate) (PMMA) used as internal standards for accurate mass measurements were from Sigma-Aldrich. For the synthesis of the oligomers, 4-amino-2,2,6,6-tetramethylpiperidine-1-oxyl (4-amino TEMPO, TCI, 97%), 3-amino-2,2,5,5-tetramethyl-1-pyrrolidinyloxy (3-amino proxyl, Acros Organics, 99%), tris(2-dimethylaminoethyl)amine ($Me_6$TREN, Alfa Aesar, >99%), trifluoroacetic acid (TFA, Sigma-Aldrich, 99%), piperidine (Sigma-Aldrich, 99%), potassium carbonate (Prolabo, 99%), *N*-diisopropylethylamine (DIPEA, Alfa Aesar, 99%), dichloromethane (DCM, Carlo Erba, 99.9%), tetrahydrofuran (THF, Aldrich, 99%, stabilized with BHT), and anhydrous dimethyl sulfoxide (DMSO, Aldrich, >99.6%) were used as received. Copper(I) bromide (Sigma-Aldrich, 98%) was washed with glacial acetic acid, filtered, washed with ethanol, and dried. 2-Bromoisobutyric anhydride **a-1** and 2-bromopropionic anhydride **a-0** were synthesized as reported in the literature.[11,21] Fmoc-Gly-Wang resin (0.7 mmol $g^{-1}$ loading) was purchased from Novabiochem/Merck, and regular Wang resin (0.7 mmol $g^{-1}$ loading) was from IRIS Biotech. As described in a previous publication,[11] the Fmoc-Gly-Wang was first deprotected with piperidine to afford a primary amine function as depicted as $\mathbf{R_wG}$ in Figure 1. The regular Wang resin $\mathbf{R_w}$ exhibits hydroxy functions that can also react with brominated anhydrides (Figure 1).[21,22] However, in that case, step (i) was repeated twice in order to obtain quantitative functionalization. Afterward, the oligomer synthesis is performed as described below.

**Oligomer Synthesis: General Procedure for Step (i).** Step (i) is the reaction of a primary amine with a symmetric noncyclic anhydride. The optimized reaction conditions for reacting an amine with anhydrides **a-0** or **a-1** are not identical.[11] For **a-1**, $K_2CO_3$ is used as a base. However, the mixture of **a-0** and $K_2CO_3$ forms a gel in THF and leads to incomplete coupling reactions. Thus, DIPEA is used instead of $K_2CO_3$ for reactions involving **a-0**. Typically, the anhydride (5 equiv as compared to resin loading) and the base (18 equiv) were added to a fritted funnel for solid-phase synthesis containing amino-functionalized resin beads. Afterward, 4 mL of THF was added, and the mixture was shaken for 50 min at RT. After completion, the solution was drained out from the fritted funnel. For steps involving **a-1**, the beads were washed with MeOH/$H_2O$ (1:1) to remove residual $K_2CO_3$ and afterward with THF. For steps involving **a-0**, the beads were washed several times with THF to remove the excess reagents.

**Oligomer Synthesis: General Procedure for Step (ii).** Step (ii) is a radical coupling reaction involving either 4-amino TEMPO (T) or 3-amino proxyl (P). Since the latter nitroxide was found to be slightly less reactive than the former, a higher excess of catalyst was used for steps involving P. Typically, the nitroxide (6 equiv as compared to resin loading) and $Me_6$TREN (3.3 or 4 equiv for T and P, respectively) were dissolved in 4 mL of anhydrous DMSO and were placed into a fritted funnel containing Br-functionalized resin beads. The funnel was sealed, and the mixture was purged with argon for 10 min. Then, CuBr (3 or 3.5 equiv for T and P, respectively) was rapidly added. The mixture was shaken for about 30 min under an inert atmosphere. After reaction, the solution was drained out from the fritted funnel, and the beads were washed with THF. It is important to mention that the efficiency of this reaction is reduced after performing several iterations on the resin. Thus, a microwave synthesizer (CEM Liberty 1TM) was used for increasing the yields. Typically, the reactions were irradiated at 150 W of microwave power at 40 °C for about 90 min. For T-based polymers, the microwave was used from step six and beyond, whereas for P-based polymers the microwave was used starting at step four.

**Oligomer Synthesis: General Procedure for Step (iii).** Cleavage of the poly(alkoxyamine amide)s from the resin was performed in TFA/DCM solution (1/1) for 2 h as previously described.[11] After reaction, the solution was filtered, concentrated, and precipitated in cold diethyl ether. The precipitate was redissolved in THF, and small amounts of insoluble resin fragments were separated by filtration. The filtrate was concentrated, and the oligomers were precipitated another time in diethyl ether. Trimers cannot be precipitated and were isolated by removing solvent and TFA. All the other higher oligomers were isolated as white solids with the exception


DOI: 10.1021/acs.macromol.5b01051
*Macromolecules* XXXX, XXX, XXX−XXX

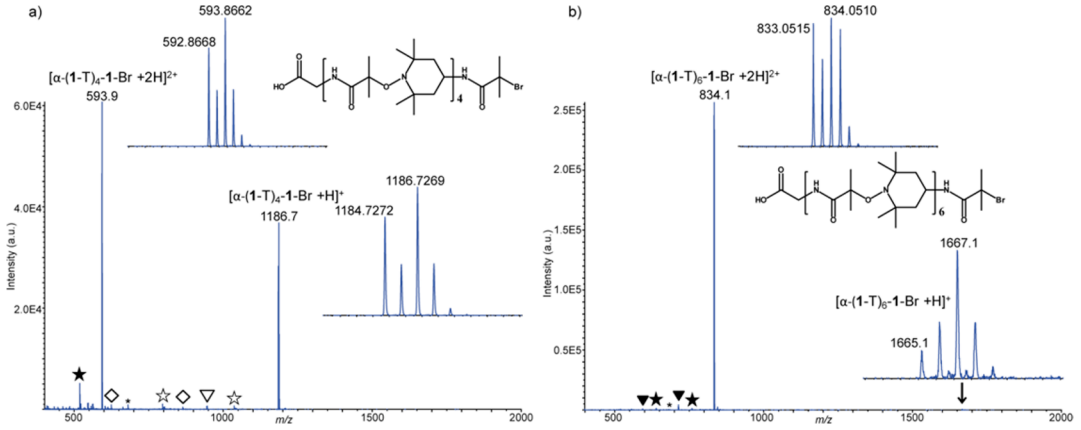


**Figure 2.** ESI mass spectrum of (a) $\alpha$-[**1**-T]$_4$-**1**-Br observed as a singly ($m/z$ 1184.7/1186.7) and a doubly ($m/z$ 592.9/$m/z$ 593.9) protonated molecule and (b) $\alpha$-[**1**-T]$_6$-**1**-Br observed as a singly ($m/z$ 1665.1/1667.1) and a doubly ($m/z$ 833.1/834.1) protonated molecule. Insets: details of the isotopic pattern of major ions, with $m/z$ values accurately measured for the two main isotopic forms (with $^{79}$Br or $^{81}$Br), and structure of the studied molecule. Peaks annotated by symbols designate impurities in the +1 (open) or +2 (filled) charge state (see text for detailed assignment).

of the pentamer containing P units, which was recovered as a viscous liquid.

**Mass Spectrometry.** High-resolution MS and MS/MS experiments were performed using a QStar Elite mass spectrometer (Applied Biosystems SCIEX, Concord, ON, Canada) equipped with an ESI source operated in the positive mode (capillary voltage: +5500 V; cone voltage: +75 V). In this hybrid instrument, ions were measured using an orthogonal acceleration time-of-flight (oa-TOF) mass analyzer. In the MS mode, accurate mass measurements were performed using reference ions from a PEG or a PMMA internal standard.[23] For collision-induced dissociation (CID) experiments, precursor ions were selected in a quadrupole mass analyzer prior to entering a collision cell filled with nitrogen, and products ions were measured in the oa-TOF. The precursor ion was used as the reference for accurate measurements of product ions in MS/MS spectra. In this instrument, air was used as nebulizing gas (10 psi) while nitrogen was used as curtain gas (20 psi). Instrument control, data acquisition, and data processing were achieved using Analyst software (QS 2.0) provided by Applied Biosystems. Sample solutions were prepared in a methanolic solution of ammonium acetate (3 mM) and introduced in the ionization source with a syringe pump (flow rate: 10 $\mu$L min$^{-1}$).

**Ion Mobility Spectrometry.** Traveling wave ion mobility mass spectrometry (TWIMS-MS) experiments were performed with a Waters Synapt G2 HDMS quadrupole/time-of-flight (QTOF) tandem mass spectrometer (Manchester, UK). TWIMS-MS spectra were recorded in the 50−1200 $m/z$ range, with trap bias dc voltage of 35 V, wave velocity of 600 m s$^{-1}$ and wave height of 40 V, helium cell gas flow of 180 mL min$^{-1}$, and the TWIMS cell operated at 3.45 mbar of $N_2$. TWIMS-MS/MS experiments were performed using argon as the collision gas. Samples were introduced at a 10 $\mu$L min$^{-1}$ flow rate in the ESI source operated in the positive mode (capillary voltage: +2.8 kV; sampling cone voltage: +20 V) under a desolvation gas ($N_2$) flow of 100 L h$^{-1}$ heated at 35 °C. Data analyses were conducted using the MassLynx 4.1 and DriftScope 2.1 programs provided by Waters.

## RESULTS AND DISCUSSION

**Electrospray Mass Spectrometry.** In contrast to usual synthetic (co)polymers, where molecules are distributed in terms of molar mass, chemical composition, molecular architecture, and concentration, the synthetic strategy implemented here aimed at producing samples containing a single type of species with a defined sequence. Moreover, as described in the Introduction, a message can be "written" in the oligomers using two amide synthons of the chains (i.e., **0** = 71.0 Da and **1**= 85.1 Da) as a binary language. Using such a **0**/**1** encoding system, a large variety of sequences can be written in rather short chains. Electrospray ionization (ESI) was then perfectly suited to generate gas phase ions from these co-oligomers, ensuring a soft ionization process while maintaining simple mass spectra in spite of multiple charging, as illustrated in Figure 2 with the examples of the $\alpha$-[**1**-T]$_4$-**1**-Br and $\alpha$-[**1**-T]$_6$-**1**-Br molecules (with $\alpha$: HOOC−CH$_2$).

In the mass spectrum obtained after ESI of $\alpha$-[**1**-T]$_4$-**1**-Br (Figure 2a), two major signals corresponding to the protonated species in the +1 ($m/z$ 1186.7) and +2 ($m/z$ 593.9) charge state were observed. The longer chain in $\alpha$-[**1**-T]$_6$-**1**-Br probably accounts for its most favored +2 charge state, with the doubly charged co-oligomer at $m/z$ 834.1 being more than 500 times more abundant than the singly protonated molecule at $m/z$ 1667.1 (Figure 2b). Both mass spectra showed that these samples were highly monodisperse, with only very minor additional signals indicating the presence of impurities (designated with filled or open symbols in Figure 2). Structural characterization of these synthesis byproducts is detailed in a later section of this article. In contrast to these ESI-MS data, numerous additional peaks corresponding to fragments were observed in MALDI-MS (Figure S1, Supporting Information), highlighting the need for a very soft ionization process to produce intact gas phase ionic species from these fragile molecules. The isotopic pattern of major ions in Figure 2 was consistent with the presence of a bromine atom in the ionized species, and accurate mass measurements further validated the assignments with relative errors below 1 ppm for [$\alpha$-[**1**-T]$_4$-**1**-Br + 2H]$^{2+}$ ($C_{58}H_{108}N_9O_{11}Br^{2+}$, $m/z_{th}$ 592.8670/593.8669), [$\alpha$-[**1**-T]$_4$-**1**-Br + H]$^+$ ($C_{58}H_{107}N_9O_{11}Br^+$, $m/z_{th}$ 1184.7268/1186.7264), and [$\alpha$-[**1**-T]$_6$-**1**-Br + 2H]$^{2+}$ ($C_{84}H_{156}N_{13}O_{15}Br^{2+}$, $m/z_{th}$ 833.0508/834.0512).

**Dissociation Mechanisms.** From the synthesis viewpoint, the encoded molecules are described as co-oligomers composed of **1** and **0** units spaced by a T nitroxide and holding a carboxymethyl moiety as the $\alpha$ end-group and bromine as the $\omega$ termination (Scheme 1, top). However, owing to their particular dissociation behavior (*vide infra*), an alternative description was adopted for a more convenient designation of product ions generating during MS/MS (Scheme 1, bottom). Accordingly, for the purpose of fragment nomenclature, encoded molecules were depicted as chains of **X**-T comonomers (with **X** = **0** or **1**) holding the original $\alpha$ end-group and capped by **X**-Br.


DOI: 10.1021/acs.macromol.5b01051
*Macromolecules* XXXX, XXX, XXX−XXX

**Scheme 1. Description of the 0/1 Encoded Co-oligomers from the Synthesis (Top) and from the MS/MS (Bottom) Viewpoints (R = H or $CH_3$ for 0 or 1, Respectively, and X = 0 or 1)**

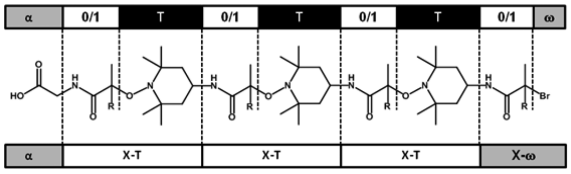


To evaluate the specificity of MS/MS dissociation, and hence its relevance for a sequencing approach, the three co-oligomers composed of two **0** and one **1** units (namely, $\alpha$-**0**-T-**0**-T-**1**-Br, $\alpha$-**0**-T-**1**-T-**0**-Br, and $\alpha$-**1**-T-**0**-T-**0**-Br) were first submitted to CID. Activation of these $m/z$ 676.3 protonated molecules gave rise to very simple, but different, MS/MS spectra depending of the comonomeric sequence in the dissociating precursor (Figure 3, left). In each spectrum, two main product ions were observed, which $m/z$ value revealed the homolytic cleavage of each C−ON bond between a coding unit and the T spacer, as depicted by the fragmentation scheme associated with each spectrum (Figure 3, right). When considering **X**-T moieties as the building blocks of the dissociating precursors (Scheme 1, bottom), the C−ON bond is the third one in any monomer when counting from the left-hand to the right-hand side, while it is the second one when numbering bonds from right to left (and not counting bonds involved in the T cycle). According to the nomenclature established by Wesdemiotis et al. for synthetic polymer fragments,[17] product ions still holding the $\alpha$ end-group after cleavage of a C−ON bond were named c (i.e., the third letter of the alphabet) while complementary fragments holding the **X**-$\omega$ termination were named y (i.e., the second letter starting from the end of the alphabet). Superscripted "•" and "+" signs were added to these two letters to account for the distonic character of these protonated radicals, and the number of partial or entire **X**-T units was indicated as a subscript. Accordingly, the two product ions

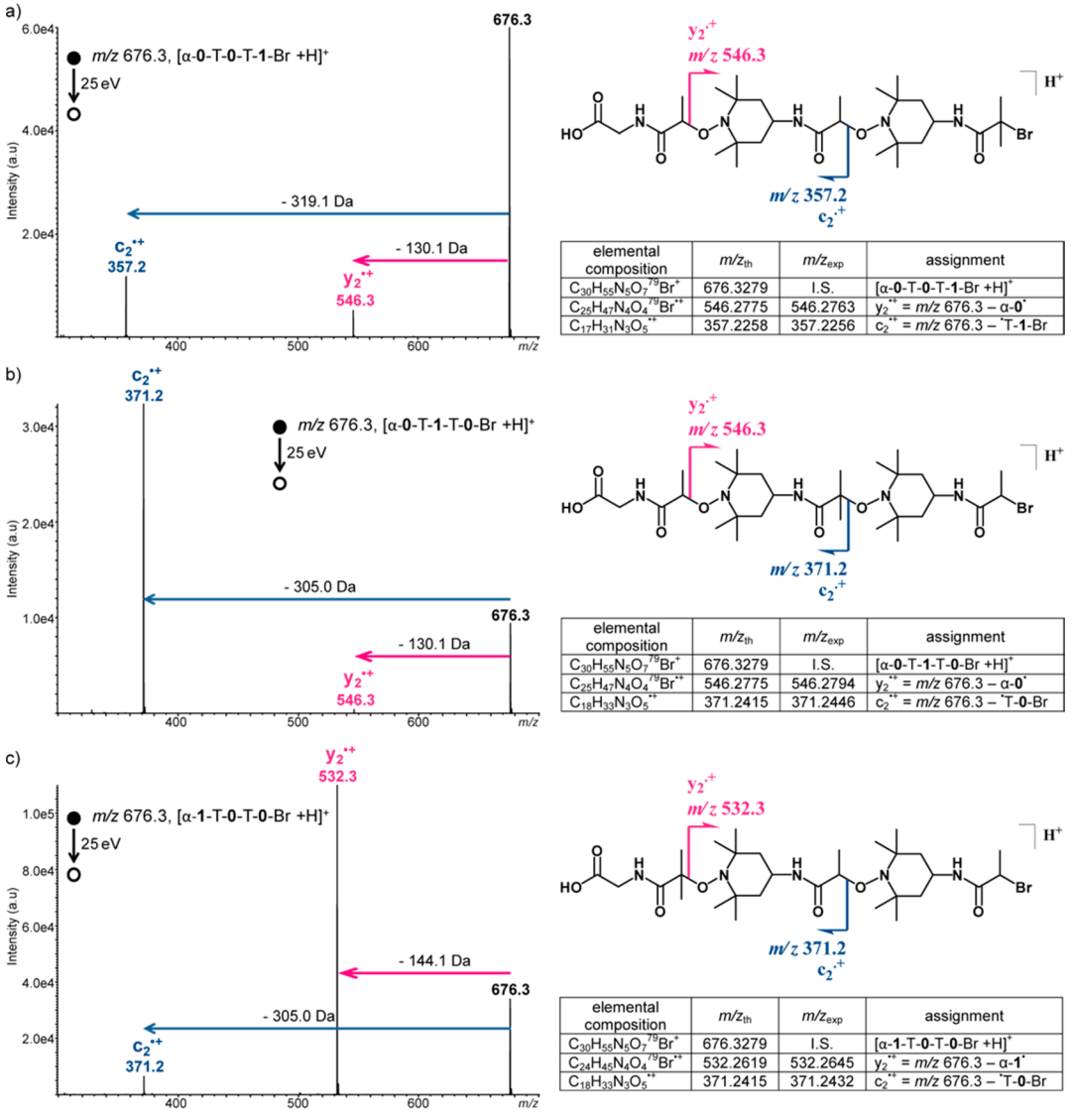


| elemental composition | $m/z_{th}$ | $m/z_{exp}$ | assignment |
|---|---|---|---|
| $C_{30}H_{55}N_5O_7{}^{79}Br^+$ | 676.3279 | I.S. | [α-**0**-T-**0**-T-**1**-Br +H]$^+$ |
| $C_{25}H_{47}N_4O_4{}^{79}Br^{\bullet+}$ | 546.2775 | 546.2763 | $y_2^{\bullet+}$ = $m/z$ 676.3 – α-**0**$^\bullet$ |
| $C_{17}H_{31}N_3O_5^{\bullet+}$ | 357.2258 | 357.2256 | $c_2^{\bullet+}$ = $m/z$ 676.3 – $^\bullet$T-**1**-Br |

| elemental composition | $m/z_{th}$ | $m/z_{exp}$ | assignment |
|---|---|---|---|
| $C_{30}H_{55}N_5O_7{}^{79}Br^+$ | 676.3279 | I.S. | [α-**0**-T-**1**-T-**0**-Br +H]$^+$ |
| $C_{25}H_{47}N_4O_4{}^{79}Br^{\bullet+}$ | 546.2775 | 546.2794 | $y_2^{\bullet+}$ = $m/z$ 676.3 – α-**0**$^\bullet$ |
| $C_{18}H_{33}N_3O_5^{\bullet+}$ | 371.2415 | 371.2446 | $c_2^{\bullet+}$ = $m/z$ 676.3 – $^\bullet$T-**0**-Br |

| elemental composition | $m/z_{th}$ | $m/z_{exp}$ | assignment |
|---|---|---|---|
| $C_{30}H_{55}N_5O_7{}^{79}Br^+$ | 676.3279 | I.S. | [α-**1**-T-**0**-T-**0**-Br +H]$^+$ |
| $C_{24}H_{45}N_4O_4{}^{79}Br^{\bullet+}$ | 532.2619 | 532.2645 | $y_2^{\bullet+}$ = $m/z$ 676.3 – α-**1**$^\bullet$ |
| $C_{18}H_{33}N_3O_5^{\bullet+}$ | 371.2415 | 371.2432 | $c_2^{\bullet+}$ = $m/z$ 676.3 – $^\bullet$T-**0**-Br |

**Figure 3.** Left: ESI-MS/MS spectra of the monoisotopic $m/z$ 676.3 precursor ion in (a) [$\alpha$-**0**-T-**0**-T-**1**-Br + H]$^+$, (b) [$\alpha$-**0**-T-**1**-T-**0**-Br + H]$^+$, and (c) [$\alpha$-**1**-T-**0**-T-**0**-Br + H]$^+$, recorded at the same 25 eV collision energy (laboratory frame). Right: structures, dissociation schemes, and accurate mass measurements (I.S.: internal standard) of product ions for each species.



DOI: 10.1021/acs.macromol.5b01051
*Macromolecules* XXXX, XXX, XXX−XXX

observed in each MS/MS spectrum of Figure 3 were $c_2^{\bullet+}$ and $y_2^{\bullet+}$.

On the one hand, formation of the $c_2^{\bullet+}$ product ion occurred after the precursor ion has eliminated the $^{\bullet}$T-**X**-$\omega$ radical, which mass is 305.1 Da when **X** = **0** or 319.1 Da when **X** = **1**. On the other hand, the $y_2^{\bullet+}$ product ion was formed after the precursor ion has lost the $\alpha$-**X**$^{\bullet}$ radical, which mass is 130.1 Da when **X** = **0** or 144.1 Da when **X** = **1**. These assignments were supported by MS/MS data recorded for the protonated molecules containing the $^{81}$Br which showed that, in contrast to $c_2^{\bullet+}$, all $y_2^{\bullet+}$ fragments were detected with a +2 $m/z$ shift (Figure S2, Supporting Information) and further validated by accurate mass data shown in the right-hand side of Figure 3. Knowing the number and the nature of the constituting coding units from the mass of the precursor ion, this unique fragmentation behavior allowed these three isobaric co-oligomers to be clearly distinguished and their sequence to be unequivocally determined.

Interestingly, each C−ON bond homolysis did not produce the pair of complementary fragments (i.e., $y_2^{\bullet+}/c_1^{\bullet+}$ and $y_1^{\bullet+}/c_2^{\bullet+}$) that could have been expected from such a charge-remote reaction. Instead, only the largest radicals were detected as protonated species: the nitroxide radical containing the **X**-$\omega$ end-group (i.e., $y_2^{\bullet+}$) formed upon cleavage of the first C−ON bond and the carbon-centered radical containing the $\alpha$ end-group (i.e., $c_2^{\bullet+}$) generated after cleavage of the second one. This result could be rationalized by considering that although not directly involved in the dissociation reaction, the adducted proton had an influence on the occurrence of this bond cleavage. In the case of synthetic polymers prepared by nitroxide-mediated polymerization, protonation of the nitrogen atom of the nitroxide termination was demonstrated to induce an increase of the dissociation energy of the C−ON bond between the nitroxide end-group and the last monomer, hence preventing its spontaneous cleavage.[24] Accordingly, the $y_2^{\bullet+}$ product ion would be generated only from precursor ions holding the proton on the nitroxide nitrogen in the second T moiety, whereas formation of the $c_2^{\bullet+}$ fragment would occur from those precursors with the proton adducted to the first T moiety. Moreover, relative abundance of the $y_2^{\bullet+}$ and $c_2^{\bullet+}$ product ions was observed to vary as a function of the precursor ion structure, revealing that relative rate of the two competing C−ON bond cleavages was sequence-dependent. A direct correlation could be established between the rate of the C−ON bond cleavage and the stability of the carbon-centered radical generated during this homolytic reaction. In the case of [$\alpha$-**0**-T-**1**-T-**0**-$\omega$ + H]$^+$, the secondary $\alpha$-**0**$^{\bullet}$ carbon-centered radical formed upon cleavage of the first C−ON bond is less stable than the tertiary $\alpha$-**0**-T-**1**$^{\bullet}$ radical generated after homolysis of the second one, accounting for the lower abundance of $y_2^{\bullet+}$ as compared to $c_2^{\bullet+}$ (Figure 3b). Similar considerations regarding [$\alpha$-**1**-T-**0**-T-**0**-$\omega$ + H]$^+$ explained the higher abundance of the $y_2^{\bullet+}$ product ion, formed after the release of the tertiary $\alpha$-**1**$^{\bullet}$, compared to $c_2^{\bullet+}$ which is the protonated secondary $\alpha$-**1**-T-**0**$^{\bullet}$ radical (Figure 3c). Finally, the relative stability of the two secondary carbon-centered radicals, $\alpha$-**0**$^{\bullet}$ and $\alpha$-**0**-T-**0**$^{\bullet}$ generated after homolysis of the first and second C−ON bonds in [$\alpha$-**0**-T-**0**-T-**1**-$\omega$ + H]$^+$ could be correlated to their relative size, accounting for $c_2^{\bullet+}$ being slightly more abundant than $y_2^{\bullet+}$ (Figure 3a). The higher rate of reactions generating a tertiary carbon-centered radical also accounts for the lower survival yield of the precursor ions observed in Figures 3b,c compared to Figure 3a.

Overall, the three $\alpha$-**0**-T-**0**-T-**1**-Br, $\alpha$-**0**-T-**1**-T-**0**-Br, and $\alpha$-**1**-T-**0**-T-**0**-Br isomeric molecules were unambiguously distinguished based on their CID pattern. Precursor ions were observed to dissociate via competitive pathways consisting of homolytic cleavage of all fragile C−ON bonds between a T spacer and the preceding coding unit, hence allowing a straightforward sequencing of the encoded copolymers.

**MS/MS Sequencing Rules.** Longer encoded chains were then subjected to dissociation experiments to evaluate the extent of the sequence coverage as the number of comonomers increases. The CID spectrum of the $\alpha$-**1**-T-**1**-T-**1**-T-**0**-T-**1**-$\omega$ species was studied based on the dissociation mechanisms previously established for encoded trimers (Figure 4). This co-oligomer contained four C−ON bonds expected to be cleaved upon activation.

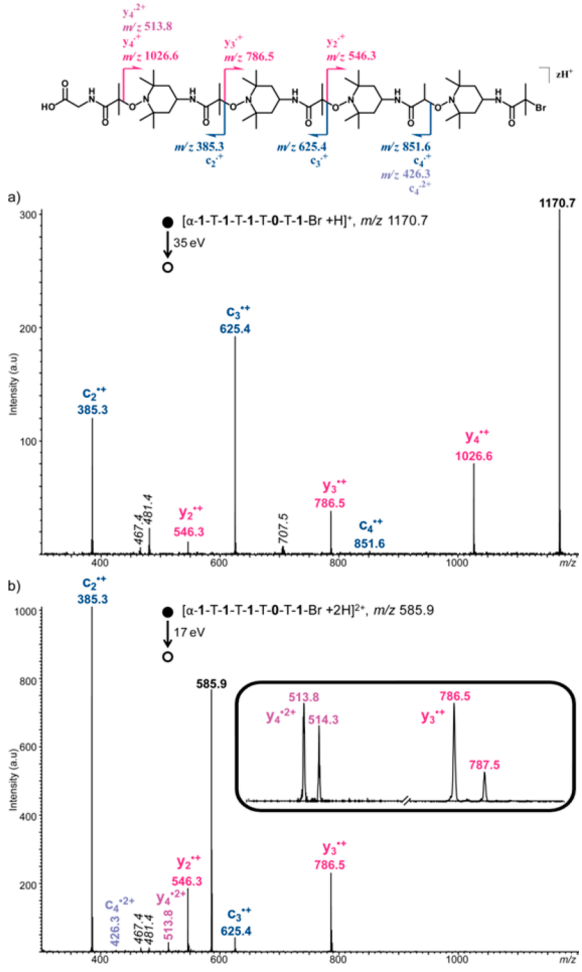


**Figure 4.** MS/MS spectra of $\alpha$-**1**-T-**1**-T-**1**-T-**0**-T-**1**-Br co-oligomer adducted with (a) one proton at $m/z$ 1170.7 (collision energy: 35 eV) or (b) two protons at $m/z$ 585.9 (collision energy: 17 eV). Top: sequencing dissociation scheme. Inset: details of the isotopic pattern of $y_4^{\bullet 2+}$ and $y_3^{\bullet+}$, which allow the $z$ charge state of each fragment to be determined from the $1/z$ distance measured between isotopic peaks.

As shown in Figure 4a, the two largest product ions at $m/z$ 1026.6 and $m/z$ 851.6 were formed after the $m/z$ 1170.7 protonated precursor has eliminated the $\alpha$-**1**$^{\bullet}$ (144.1 Da) and $^{\bullet}$T-**1**-$\omega$ (319.1 Da) radicals and were hence designated as $y_4^{\bullet+}$ and $c_4^{\bullet+}$, respectively. Lower congeners in each series were then observed as peaks spaced by 226.2 $m/z$ (**0**-T) or 240.2 $m/z$ (**1**-


DOI: 10.1021/acs.macromol.5b01051
Macromolecules XXXX, XXX, XXX−XXX

T), consistent with the expected sequence: on the one hand, $y_3^{\bullet+}$ at $m/z$ 786.5 (= 1026.6 − 240.2) and $y_2^{\bullet+}$ at $m/z$ 546.3 (= 786.5 − 240.2) allowed the left side of the co-oligomer to be reconstructed as $\alpha$-**1**-T-**1**-T-**1**; on the other hand, $c_3^{\bullet+}$ at $m/z$ 625.4 (= 851.6 − 226.2) and $c_2^{\bullet+}$ at $m/z$ 385.3 (= 625.4 − 240.2) confirmed the right side of the co-oligomer to be T-**1**-T-**0**-T-**1**-$\omega$. These results showed that all alkoxyamine linkages in the precursor ion indeed experienced homolysis.

As depicted in the dissociation scheme of Figure 4, cleavage of all these C−ON bonds, but the first and the last ones, produced pairs of complementary fragments, that is, $c_2^{\bullet+}/y_3^{\bullet+}$ and $c_3^{\bullet+}/y_2^{\bullet+}$ after homolysis of the second and the third bonds, respectively. Relative abundance of product ions in Figure 4a can be explained using the same assertions previously proposed for trimers (*vide supra*). On the one hand, relative abundance of $c_i^{\bullet+}$ fragments is directly correlated to the relative stability of these protonated carbon-centered radicals: the protonated secondary radical $c_4^{\bullet+}$ is the least intense while $c_3^{\bullet+}$ is the most abundant protonated tertiary radical due to size effect. On the other hand, the observed decreasing intensity trend observed for $y_i^{\bullet+}$ fragments (all formed upon release of tertiary carbon-centered radicals) as their size decreases can be accounted for based on the protonation state of the precursor ion. Statistically, the $y_4^{\bullet+}$ product ion should be more prominent as it can be generated from precursor ions with the proton adducted to the second, third, or fourth nitroxide, whereas $y_3^{\bullet+}$ can be formed only from those precursors holding the proton at the third or fourth T moieties and $y_2^{\bullet+}$ can solely appear if the fourth T is protonated.

Overall, the competitive homolytic cleavages of the C−ON bonds occurring during CID of protonated poly(alkoxyamine amide)s allowed their complete sequencing in a straightforward manner. Despite the increase of the chain length, no alternative dissociation reaction was observed to efficiently compete with the low-energy demanding homolytic cleavage of the C−ON bonds. Moreover, the nature of the coding units has no influence on this main fragmentation process. In contrast to the smallest oligomers discussed previously, a few additional signals (designated by italicized $m/z$ values in Figure 4) were observed beside the $c_i^{\bullet+}$ and $y_i^{\bullet+}$ fragments. These secondary product ions were found to be internal fragments; that is, they did no longer contain any original end-group of the dissociating precursor. Peaks at $m/z$ 707.5 and $m/z$ 481.4 were assigned to secondary fragments formed after the release of $\alpha$-**1**$^{\bullet}$ (144.1 Da) from $c_4^{\bullet+}$ and $c_3^{\bullet+}$, respectively, while the signal at $m/z$ 467.4 was found to correspond to the species formed after the release of $\alpha$-**1**-T-**1**$^{\bullet}$ (384.2 Da) from $c_4^{\bullet+}$ (Table S1, Supporting Information). These reactions were proposed to occur according to a radical-driven mechanism to generate protonated cyclic species (Scheme S1, Supporting Information). As they were composed of different pieces of the original chain (T-**1**-T-**0** for $m/z$ 467.4, T-**1**-T-**1** for $m/z$ 481.4, and T-**1**-T-**1**-T-**0** for $m/z$ 707.5), these internal fragments cannot be used for sequencing purposes but could still be utilized to support the commoner sequence revealed by primary product ions. For example, the presence of both $m/z$ 467.4 and $m/z$ 481.4 internal fragments respectively indicated the occurrence of the **1**-T-**0** and **1**-T-**1** structural motifs in the studied chain.

As the $\alpha$-**1**-T-**1**-T-**1**-T-**0**-T-**1**-Br co-oligomer was also observed in the +2 charge state in ESI-MS, the $m/z$ 585.9 doubly protonated molecule was submitted to CID to study any influence of the charge state on the dissociation behavior established for singly charged species. As can be seen in Figure 4b (and validated by accurate mass measurements reported in Table S2, Supporting Information), fragmentation pathways proceeded the same way as for the singly charged precursor, but the largest fragments were mainly detected as doubly protonated species, i.e., $c_4^{\bullet 2+}$ and $y_4^{\bullet 2+}$. By slightly decreasing the resolving power of the quadrupole mass analyzer in the Q-TOF instrument, the two first isotopic forms of the precursor ion can be simultaneously selected and subjected to CID, hence allowing the charge state of product ions to be easily deciphered from their isotopic pattern (as illustrated in the inset of Figure 4b). These MS/MS experiments showed that full sequence coverage was still achieved in spite of the increase of the precursor ion charge state, offering promising perspectives for the sequencing of larger co-oligomers.

To further evaluate the robustness of the MS/MS sequencing, we investigated the effect of the nature of the $\alpha$-chain-end on the sequencing rules. An oligomer with a different $\alpha$ end-group (further called $\alpha'$) was synthesized. This type of polymer is obtained using a classical Wang resin $\mathbf{R_w}$ (Figure 1) instead of the glycine-loaded Wang resin $\mathbf{R_WG}$ that has been used in our previous work.[11] In this case, the first anhydride (**a-0** or **a-1**) is reacted with the hydroxy group of the resin to afford a cleavable ester linkage. Strictly speaking, the resulting adduct is not a coding unit **0** or **1** because it does not contain an amide bond as defined in Scheme 1. Thus, after cleavage from the resin, it becomes a carboxyalkyl $\alpha'$-end-group that is directly connected to a T moiety. This design is different from the one of the polymers synthesized on $\mathbf{R_WG}$, in which the $\alpha$-moiety is connected to a **0**/**1** coding unit. As exemplified in Figure 5a with the case of the $\alpha'$-T-**0**-T-**1**-T-**0**-Br co-oligomer, where $\alpha'$ is a carboxyisopropyl moiety, the main dissociation pathways still proceeded via C−ON bond homolysis, giving rise

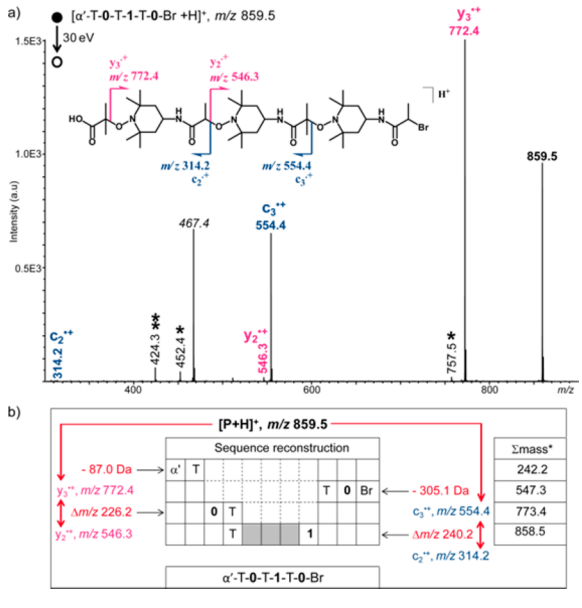


**Figure 5.** (a) MS/MS spectra (collision energy: 30 eV) of the protonated $\alpha'$-T-**0**-T-**1**-T-**0**-Br co-oligomer at $m/z$ 859.5, with its sequencing dissociation scheme as an inset. (b) Reconstruction of the $[P + H]^+$ precursor ion sequence from the left- to the right-hand side using $y_i^{\bullet+}$ product ions and the other way round using $c_i^{\bullet+}$ product ions. *Summing the mass of each moiety revealed by the $m/z$ distance measured between peaks allows one to connect the two growing sequence pieces when reaching the molecular mass of the dissociating co-oligomer.



DOI: 10.1021/acs.macromol.5b01051
*Macromolecules* XXXX, XXX, XXX−XXX

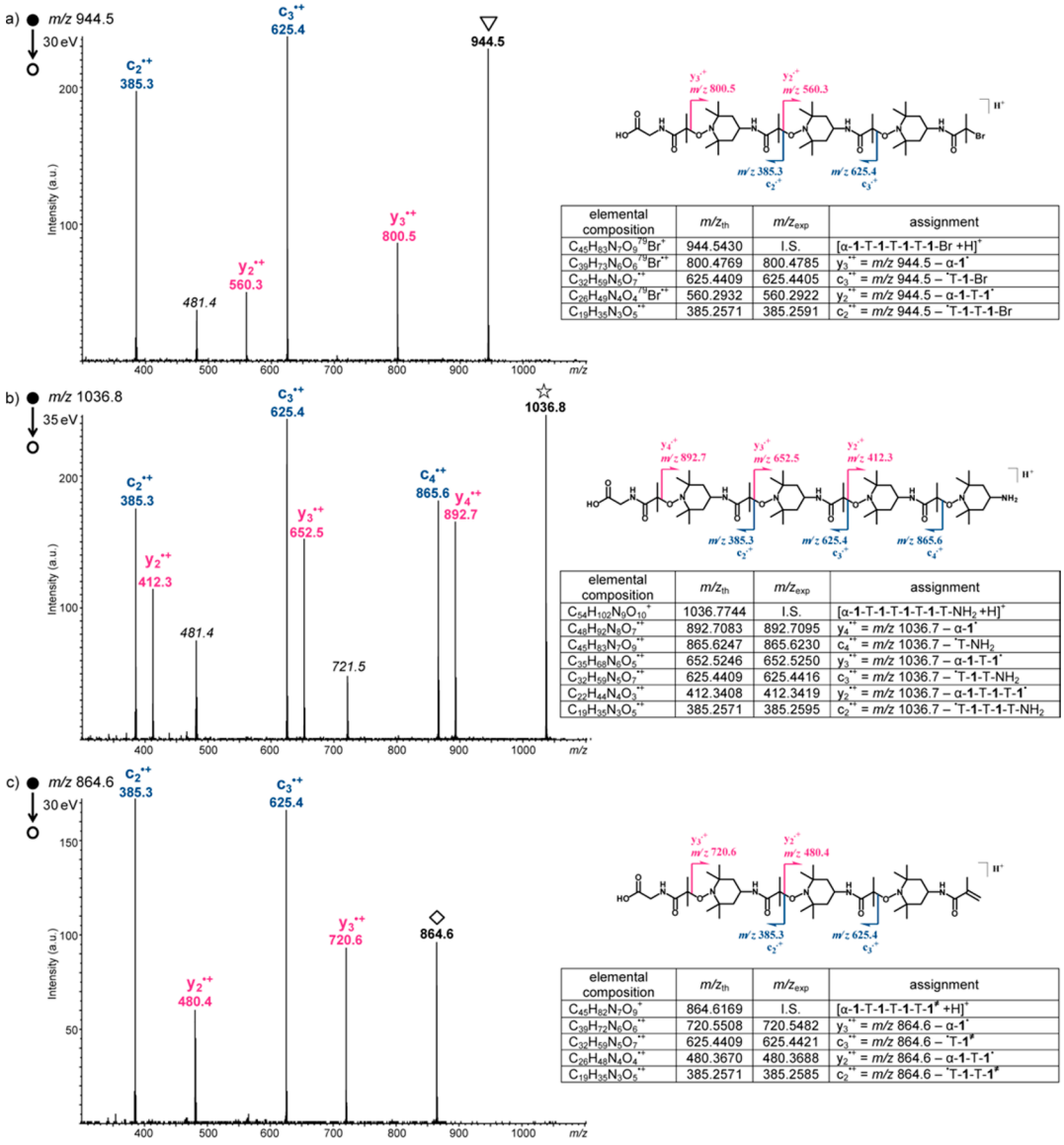


**Figure 6.** MS/MS spectra of impurities detected in the ESI mass spectrum of α-[**1**-T]$_4$-**1**-Br at (a) *m/z* 944.5 (open triangle), (b) *m/z* 1036.8 (open star), and (c) *m/z* 864.6 (open diamond). Symbols refer to Figure 2. Italicized *m/z* values designate internal fragments.

to the two $c_i^{\bullet+}$ and $y_i^{\bullet+}$ product ion series that allowed the co-oligomer sequence to be reconstructed (Figure 5b).

The *m/z* 467.4 internal fragment confirmed that the precursor ion mainly exhibited alternating **0**/**1** units. As compared to co-oligomer with the α moiety connected to a **0**/**1** coding unit, new secondary fragments were generated during CID of the protonated α′-T-**0**-T-**1**-T-**0**-Br. The *m/z* value measured for product ions designated by one asterisk in Figure 5a suggested that species containing the α′ termination had experienced a 102.0 Da neutral loss (*m/z* 859.5 → *m/z* 757.5, *m/z* 554.4 → *m/z* 452.4). As depicted in Scheme S2 (Supporting Information), the close proximity of the first T moiety with the carboxylic acid group in α′ would allow a 1,5 transfer of the acidic proton to the nitroxide nitrogen atom, conducting to the combined release of carbon dioxide (44.0 Da) and acetone (58.0 Da). Similarly, the α′ termination would be involved in the mechanism leading to the formation of the secondary *m/z* 424.3 product ion (designated by two asterisks in Figure 5a) upon dissociation of $c_3^{\bullet+}$ (Scheme S3, Supporting Information). These assignments were supported by accurate mass measurements (Table S3, Supporting Information).

In summary, MS/MS data obtained for protonated poly(alkoxyamine amide)s can be usefully employed to rapidly decipher their encoded message based on very simple sequencing rules, independent of the size and the charge state of the dissociating co-oligomer, as well as the connectivity of the initial group. Measuring the mass of the two smallest radicals released from the precursor ion allows the highest congeners of each product ion series to be identified and so the coding unit linked to each termination. Then, measuring the distance between consecutive peaks from $c_n^{\bullet+}$ down to $c_2^{\bullet+}$ and from $y_n^{\bullet+}$ down to $y_2^{\bullet+}$ allows the binary (**1**, **0**) sequence in the precursor ion to be reconstructed, starting from the ω- or α-chain-end, respectively.

**MS/MS Sequencing of Defect Sequences.** The efficiency of the sequencing methodology at characterizing the structure of unknowns was evaluated for the impurities detected with low abundance beside signals of perfect co-oligomers in Figure 2. The isotopic pattern of the signal


DOI: 10.1021/acs.macromol.5b01051
*Macromolecules* XXXX, XXX, XXX−XXX

detected at $m/z$ 944.5, designated with an open triangle in Figure 2a, indicated a brominated molecule. Applying the sequencing rules to MS/MS data obtained for this protonated molecule (Figure 6a) conducted to the following findings:

- The $m/z$ 800.5 product ion was formed after the precursor ion has eliminated the 144.1 Da $\alpha$-**1**$^{\bullet}$ radical and was hence the largest member of the $y_i^{\bullet+}$ series; the signal of the $y_{i-1}^{\bullet+}$ congener ($m/z$ 560.3) was detected at a 240.1 $m/z$ distance compared to $y_i^{\bullet+}$, allowing to complete the left-hand side sequence as $\alpha$-**1**-T-**1** ($m$ = 384.2 Da).
- The $m/z$ 625.4 product ion was formed after the precursor ion has eliminated the 319.1 Da $^{\bullet}$T-**1**-Br radical and was hence designated as the largest member of the $c_i^{\bullet+}$ series; the signal of the $c_{i-1}^{\bullet+}$ congener was detected at $m/z$ 385.2, that is, a 240.1 $m/z$ distance compared to $c_i^{\bullet+}$, allowing to complete the right-hand side sequence as T-**1**-T-**1**-Br ($m$ = 559.3 Da).
- Summing the mass of these two partial sequences led to the molecular mass of the impurity, allowing its structure to be defined as $\alpha$-**1**-T-**1**-T-**1**-T-**1**-Br.

The subscripted $i$ value in $c_i^{\bullet+}$ and $y_i^{\bullet+}$ product ions was then assigned based on the polymerization degree of this molecule. Accurate mass measurement of this protonated species was consistent with the proposed $C_{45}H_{83}N_7O_9{}^{79}Br^+$ elemental composition ($m/z_{th}$ 944.5430, $m/z_{exp}$ 944.5445) and further used to validate the composition of product ions (right-hand side of Figure 6a). Finally, the $m/z$ 481.4 internal fragment (that is, a protonated cyclic species composed two T-1 moieties) formed after the release of $\alpha$-**1**$^{\bullet}$ from the $m/z$ 625.4 $c_3^{\bullet+}$ product ion (Scheme S1 in the Supporting Information) further confirmed that only **1** coding units were involved in the sequence. As compared to the $\alpha$-[**1**-T]$_4$-**1**-Br co-oligomer targeted during synthesis of this sample, this impurity indicated that some oligomers did not undergo the last step (ii) of the sequential synthesis (see Figure 1). Byproducts exhibiting the same structure but a lower polymerization degree were also detected with low abundance in the mass spectrum of $\alpha$-[**1**-T]$_6$-**1**-Br sample (designated with filled triangles at $m/z$ 713.0 and $m/z$ 592.9 in Figure 2b), as revealed by their MS/MS data (Figures S3 and S4, Supporting Information).

Similar analysis of MS/MS data shown in Figure 6b allowed the structure of the nonbrominated impurity detected at $m/z$ 1036.8 (open star in Figure 2a) to be readily determined. On the one hand, the three members of the $y_i^{\bullet+}$ series ($m/z$ 892.7, $m/z$ 652.5, and $m/z$ 412.3) were all spaced by 240.1 $m/z$ (consistent with the sole use of **1** coding units in this synthesis process), and the largest one was obtained after the precursor ion has released $\alpha$-**1**$^{\bullet}$, conducting to a left-hand-side sequence such as $\alpha$-**1**-T-**1**-T-**1**. On the other hand, the highest member of the $c_i^{\bullet+}$ series at $m/z$ 865.6 was formed after the precursor ion has eliminated a 171.1 Da radical: owing to the 155.1 Da mass of T, this radical was assumed to be $^{\bullet}$T-NH$_2$. Lower congeners of the $c_i^{\bullet+}$ series detected at $m/z$ 625.4 and $m/z$ 385.3 allowed the sequence of this impurity to be proposed as $\alpha$-**1**-T-**1**-T-**1**-T-**1**-T-NH$_2$. This assignment was further supported by accurate mass measurements performed in the MS mode ($C_{54}H_{102}N_9O_{10}^+$: $m/z_{th}$ 1036.7744, $m/z_{exp}$ 1036.7756) and in the MS/MS mode (right-hand side of Figure 6b). This molecule was also detected as a doubly protonated species at $m/z$ 518.9 (hence designated with a filled star in Figure 2a). All minor signals designated with either open (1+) or filled (2+) stars in Figure 2 were found to have the same NH$_2$ termination (Figures S5−S7, Supporting Information) and correspond to incomplete radical coupling steps during the synthesis (i.e., oligomers formed after a step (ii) that did not react further in a subsequent step (i); see Figure 1). Finally, impurities designated with diamonds in Figure 2 could also be explained as byproducts generated during the step synthesis of poly(alkoxy(amine amide)s, as exemplified by the case of the nonbrominated species detected at $m/z$ 864.6 (Figure 6c). While this molecule was found to be composed of **1** coding units only and to hold the carboxymethyl $\alpha$ starting group (based on the analysis of $y_i^{\bullet+}$ product ions), the $c_3^{\bullet+}$ fragment at $m/z$ 625.4 revealed that the precursor ion has released a $^{\bullet}$T-Y radical of mass 239.2 Da, with a Y moiety of mass 84.1 Da, that is, 1 mass unit less than the **1** coding unit. Accordingly, this impurity was proposed to be ended by an endo-unsaturation, as depicted in the right-hand side of Figure 6c and supported by accurate mass measurements of both the dissociating precursor ($C_{45}H_{82}N_7O_9^+$: $m/z_{th}$ 864.6169, $m/z_{exp}$ 864.6195) and its product ions generated in MS/MS (right-hand side of Figure 6c). Analysis of MS/MS data obtained for the other low abundance species designated with an open diamond at $m/z$ 624.6 in Figure 2a is detailed in the Supporting Information (Figure S8). These unsaturated species are typically formed by H transfer during step (ii) of the synthesis (Figure 1).[25] This side-reaction may occur when a tertiary carbon-centered radical is used in step (ii), e.g., when the moiety **1**-Br is activated by copper bromide. This side-reaction is usually predominant at high temperatures (e.g., above 100 °C) but was found to be disfavored at lower temperatures.[11,13,26] The ESI results shown in Figure 2 confirm that this side-reaction is marginal in the experimental conditions used for the synthesis of sequence-coded oligo(alkoxyamine amide)s.

These few examples clearly showed that the sequencing methodology also performed well for encoded chains with different $\omega$ end-groups. As expected from any MS/MS method applied to synthetic polymers, it also allowed unknown terminations to be structurally characterized, providing relevant information about side-reactions taking place to a minor extent during the iterative synthesis of poly(alkoxyamine amide)s.

**Alternative Monomer Codes.** Two amide moieties with 71.0 and 85.1 Da mass were used in the previous sections as **0** and **1** coding units, respectively. This is of course an arbitrary choice among many other possibilities. As proposed in an earlier publication,[11] different types of monomer-based codes could be created using the synthesis concept shown in Figure 1. For instance, other anhydrides or nitroxides could be used to create coded sequences. Furthermore, the monomer-based code does not necessarily have to be binary but could be ternary or even more complex. However, for each new monomer, the validity of the established MS/MS sequencing rules should be assessed. Information-encoded poly(alkoxyamine amide)s were synthesized using 3-amino proxyl (P) as an alternative nitroxide instead of T in step (ii) (Figure 1). The same dissociation rules were found to apply for these polymers, as illustrated by the example of $\alpha$-**0**-P-**0**-P-**0**-P-**0**-Br in Supporting Information (Figure S9). Owing to the 141.1 Da mass of the P moiety, the largest member of the $c_i^{\bullet+}$ fragment was detected after the precursor ion has lost the $^{\bullet}$P-**0**-Br radical (291.1 Da), and the distance between peaks within the $c_i^{\bullet+}$ and $y_i^{\bullet+}$ product ion series corresponded to the 212.2 Da mass of P-**0**. Changing the nature of the nitroxide in the poly(alkoxyamine amide) skeleton hence simply required the mass of the new building blocks to be considered for the calculation of the mass of released radicals, opening the perspective to develop a


DOI: 10.1021/acs.macromol.5b01051
Macromolecules XXXX, XXX, XXX−XXX

computer program to operate the sequencing methodology in an automated manner. Of note, different internal fragments were detected as compared to poly(alkoxyamine amide)s involving T nitroxides. A secondary product ion at $m/z$ 415.3 was found to be formed after $c_3^{\bullet+}$ has eliminated a $C_8H_{14}NO^{\bullet}$ radical (Table S4, Supporting Information), corresponding to a net loss of one H atom compared to the elemental composition of P. A two-step mechanism was proposed to account for the release of the 2,2,5,5-tetramethyl-pyrrolin-1-oxyl radical (Scheme S4, Supporting Information), suggesting that poly(alkoxyamine amide) chains are more likely to undergo internal rearrangement when containing P instead of T.

The only case where the MS/MS sequencing methodology may become tricky is the particular scenario of isobaric molecules containing both T and P nitroxides. Indeed, as the methodology is mainly based on the $m/z$ difference measured between product ions generated upon homolytic cleavage of the C−ON bonds, any chemical block between any two C−ON bonds is identified based on its whole mass, not the individual mass of the nitroxide and the coding unit inside this block. As a result, since T and P only differ by a methylene moiety as do **1** and **0**, the mass coincidence of T-**0** and P-**1** blocks does not allow them to be distinguished in MS/MS spectra. Such a case is illustrated by the examples of $\alpha$-**1**-T-**1**-T-**1**-T-**0**-Br and $\alpha$-**1**-T-**1**-T-**1**-P-**1**-Br co-oligomers, both detected at $m/z$ 930.5 as protonated molecules and displaying the same product ions (Figure S10, Supporting Information). The main difference between these two CID spectra is the relative abundance of $c_3^{\bullet+}$, which could be explained based on the relative stability of the radicals ($^{\bullet}$T-**1**-Br > $^{\bullet}$P-**1**-Br) to be expelled from the precursor ion to form this specific fragment. However, too many factors might influence the relative abundance of product ions in MS/MS spectra of poly(alkoxyamine amide)s, particularly for increasing size chains, so safe sequencing results cannot rely on such subtle variations. Nevertheless, distinction of the two species could be achieved by traveling wave ion mobility spectrometry (TWIMS),[27,28] which allows ionic species to be separated based on their conformation. Figure 7

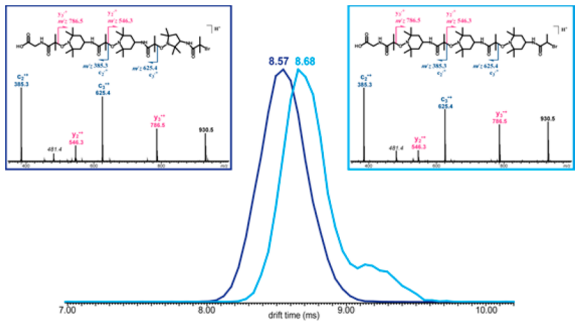


**Figure 7.** Arrival time distribution of protonated $\alpha$-**1**-T-**1**-T-**1**-P-**1**-Br (dark blue) and $\alpha$-**1**-T-**1**-T-**1**-T-**0**-Br (light blue) co-oligomers both at $m/z$ 930.5. Insets: CID spectra extracted from each peak when performing IMS-MS/MS experiments.

shows the arrival time distributions obtained when monitoring the $m/z$ 930.5 ion generated from each sample individually analyzed in ESI-IMS-MS: the lower drift time measured for the protonated $\alpha$-**1**-T-**1**-T-**1**-P-**1**-Br indicated a slightly more compact conformation of this co-oligomer as compared to $\alpha$-**1**-T-**1**-T-**1**-T-**0**-Br. This result would be consistent with the more flexible chain of P-containing molecules, as previously suspected with the specific internal fragment generated from these co-oligomers (Scheme S4, Supporting Information).

Finally, thanks to the capability of the instrument to select precursor ions prior to the mobility cell and to activate them as they exit the mobility cell, co-oligomer sequencing could still be performed after the IMS separation step, as shown by MS/MS spectra extracted from each peak when recording ESI-IMS-MS/MS experiments (insets of Figure 7).

## CONCLUSIONS

Thanks to the particular design of the studied sequence-coded oligo(alkoxyamine amide)s which contained fragile C−ON bonds between each coding unit and a nitroxide moiety, MS/MS data were usefully employed to rapidly decipher their encoded message based on very simple sequencing rules. Robustness of this tandem mass spectrometric sequential analysis of digitally encoded molecules was demonstrated for a set of different poly(alkoxyamine amide)s varying in terms of size, charge state, end-groups, and nitroxide moieties. Finally, it should be added that while the use of high-resolution mass analyzers was mandatory in this study to safely establish mechanisms governing the dissociation reactions experienced by protonated co-oligomers, the same sequence coverage was obtained in low-resolution MS/MS (Figure S11 in Supporting Information), opening the route to a broader dissemination of this analytical approach.

## ASSOCIATED CONTENT

### Supporting Information

Figures S1−S11, Schemes S1−S4, and Tables S1−S4. The Supporting Information is available free of charge on the ACS Publications website at DOI: 10.1021/acs.macromol.5b01051.

## AUTHOR INFORMATION

### Corresponding Authors

*E-mail: laurence.charles@univ-amu.fr (L.C.).
*E-mail: jflutz@unistra.fr (J.-F.L.).

### Notes

The authors declare the following competing financial interest(s): J.-F.L. is named inventor on a patent application related to this work.

## ACKNOWLEDGMENTS

L.C. acknowledges support from Spectropole, the Analytical Facility of Aix-Marseille University, by allowing a special access to the instruments purchased with European Funding (FEDER OBJ2142-3341). J.F.L. thanks the European Research Council (project SEQUENCES − ERC grant agreement no. 258593), the Cluster of Excellence Chemistry of Complex Systems (LabEx CSC), and the CNRS for financial support. The postdoc position of R.K.R. was supported by the ERC. The PhD position of C.L. is supported by the LabEX CSC.

## REFERENCES

(1) Lutz, J.-F.; Ouchi, M.; Liu, D. R.; Sawamoto, M. *Science* **2013**, *341*, 1238149.
(2) Colquhoun, H.; Lutz, J.-F. *Nat. Chem.* **2014**, *6*, 455−456.
(3) Church, G. M.; Gao, Y.; Kosuri, S. *Science* **2012**, *337*, 1628−1628.
(4) Goldman, N.; Bertone, P.; Chen, S.; Dessimoz, C.; LeProust, E. M.; Sipos, B.; Birney, E. *Nature* **2013**, *494*, 77−80.
(5) Grass, R. N.; Heckel, R.; Puddu, M.; Paunescu, D.; Stark, W. J. *Angew. Chem., Int. Ed.* **2015**, *54*, 2552−2555.
(6) Lutz, J.-F. *ACS Macro Lett.* **2014**, *3*, 1020−1023.


DOI: 10.1021/acs.macromol.5b01051
*Macromolecules* XXXX, XXX, XXX−XXX

(7) Al Ouahabi, A.; Charles, L.; Lutz, J.-F. *J. Am. Chem. Soc.* **2015**, *137*, 5629−5635.
(8) Pfeifer, S.; Zarafshani, Z.; Badi, N.; Lutz, J.-F. *J. Am. Chem. Soc.* **2009**, *131*, 9195.
(9) Trinh, T. T.; Oswald, L.; Chan-Seng, D.; Lutz, J.-F. *Macromol. Rapid Commun.* **2014**, *35*, 141−145.
(10) Trinh, T. T.; Oswald, L.; Chan-Seng, D.; Charles, L.; Lutz, J.-F. 2015, submitted.
(11) Roy, R. K.; Meszynska, A.; Laure, C.; Charles, L.; Verchin, C.; Lutz, J.-F. *Nat. Commun.* **2015**, *6*, 7237.
(12) Trinh, T. T.; Laure, C.; Lutz, J.-F. *Macromol. Chem. Phys.* **2015**, DOI: 10.1002/macp.201500072.
(13) Matyjaszewski, K.; Woodworth, B. E.; Zhang, X.; Gaynor, S. G.; Metzner, Z. *Macromolecules* **1998**, *31*, 5955−5957.
(14) Mutlu, H.; Lutz, J.-F. *Angew. Chem., Int. Ed.* **2014**, *53*, 13010−13019.
(15) Biemann, K. *Int. J. Mass Spectrom.* **2007**, *259*, 1−7.
(16) Domon, B.; Costello, C. E. *Glycoconjugate J.* **1988**, *5*, 397−409.
(17) Wesdemiotis, C.; Solak, N.; Polce, M. J.; Dabney, D. E.; Chaicharoen, K.; Katzenmeyer, B. C. *Mass Spectrom. Rev.* **2011**, *30*, 523−559.
(18) Paulick, M. G.; Hart, K. M.; Brinner, K. M.; Tjandra, M.; Charych, D. H.; Zuckermann, R. N. *J. Comb. Chem.* **2006**, *8*, 417−426.
(19) Thakkar, A.; Cohen, A. S.; Connolly, M. D.; Zuckermann, R. N.; Pei, D. *J. Comb. Chem.* **2009**, *11*, 294−302.
(20) Porel, M.; Alabi, C. A. *J. Am. Chem. Soc.* **2014**, *136*, 13162−13165.
(21) Ostmark, E.; Harrisson, S.; Wooley, K. L.; Malmstrom, E. E. *Biomacromolecules* **2007**, *8*, 1138−1148.
(22) Ohno, K.; Wong, B.; Haddleton, D. M. *J. Polym. Sci., Part A: Polym. Chem.* **2001**, *39*, 2206−2214.
(23) Charles, L. *Rapid Commun. Mass Spectrom.* **2008**, *22*, 151−155.
(24) Mazarin, M.; Girod, M.; Viel, S.; Phan, T. N. T.; Marque, S. R. A.; Humbel, S.; Charles, L. *Macromolecules* **2009**, *42*, 1849−1859.
(25) Gryn'ova, G.; Lin, C. Y.; Coote, M. L. *Polym. Chem.* **2013**, *4*, 3744−3754.
(26) Lin, W.; Huang, B.; Fu, Q.; Wang, G.; Huang, J. *J. Polym. Sci., Part A: Polym. Chem.* **2010**, *48*, 2991−2999.
(27) Giles, K.; Pringle, S. D.; Worthington, K. R.; Little, D.; Wildgoose, J. L.; Bateman, R. H. *Rapid Commun. Mass Spectrom.* **2004**, *18*, 2401−2414.
(28) Shvartsburg, A. A.; Smith, R. D. *Anal. Chem.* **2008**, *80*, 9689−9699.


DOI: 10.1021/acs.macromol.5b01051
*Macromolecules* XXXX, XXX, XXX−XXX